Energy 270 (2023) 126957

Contents lists available at ScienceDirect

Energy

journal homepage: www.elsevier.com/locate/energy

Flow distribution and heat transfer performance of two-phase flow in parallel flow heat exchange system

Ping Yang, Weihao Ling, Ke Tian, Min Zeng *, Qiuwang Wang

Key Laboratory of Thermo-Fluid Science and Engineering, Ministry of Education, Xi'an Jiaotong University, Xi'an, 710049, Shaanxi, PR China

ARTICLE INFO

Handling Editor: Petar Sabev Varbanov

Keywords:
Flow distribution
Flow boiling
Non-uniform thermal load
Parallel flow system
Heat transfer

ABSTRACT

Two-phase flow parallel heat exchange systems are widely used in solar energy collectors, nuclear reactors, air-conditioners and electronic thermal management. However, flow maldistribution in multiple channels may lead to heat transfer deterioration. In this study, a numerical model is developed to quickly predict the flow distribution and heat transfer of two-phase flow in the parallel flow system, and the maximum average relative deviation with experimental data is 4.4%. The effects of geometric parameters and non-uniform thermal load on flow and heat transfer are discussed. Decreasing the channel to header area ratio *AR* can significantly improve the flow maldistribution when *AR* is greater than 0.3. Moreover, dimensionless parameters Y_m and H are introduced to predict the worst operating condition when the heating is non-uniform. The results indicate that the mass flow rate of the channel near the low thermal load channel reduced significantly, especially the downstream channel. The 2nd channel from the inlet should be avoided being the low thermal load channel, and the maximum outlet vapor quality $(x_{out})_{max}$ is a linear function of H. If it's assumed that $(x_{out})_{max} = 1$ is the worst condition, the thermal non-uniformity dimensionless parameter H must be less than about 198 in this study.

1. Introduction

With the global energy scarcity and environmental problems aggravation, new and clean energy systems are in urgent demand [1], where high-performance and compact heat exchangers are vital technologies. Parallel flow heat exchange systems are widely used in solar energy collectors [2], nuclear reactors [3], air-conditioners and electronic thermal management among others [4]. Besides, flow boiling is always a hot issue due to the higher heat transfer coefficient and more uniform temperature compared with single-phase flow. Therefore, to improve performance and optimize design, it is essential to investigate the heat transfer characteristics of two-phase flow in the parallel flow heat exchange system.

However, flow maldistribution significantly affects the thermal performance of the parallel flow system, especially in the two-phase flow system. Therefore, a great quantity of studies on flow distribution have been carried out in the past several decades. Wang et al. [5] experimentally and numerically studied the flow distribution of single-phase flow in the heat exchangers with typical headers, and they pointed out that jet flow effects significantly affect flow maldistribution. Afterwards, Wang et al. [6] investigated the flow distribution in a parallel flow system through modified headers like trapezoidal header, baffle tubes header and so on. The results indicated that the baffle tube header could remove the vortex flow so it's best to improve flow distribution. Siddiqui et al. [7] measured the flow velocity and flow distribution in 10 channels using the particle image velocimetry (PIV) technique, and they pointed out that a U-type wider header is recommended for better flow distribution. Klugmann et al. [8] studied heat transfer and flow distribution in minigap based on visualization experiments, and they proposed a modified minigap surface to reduce the maldistribution and flow resistance. Kumar et al. [9] focused on the effect of flow maldistribution on flow boiling in the microchannel heat sink with an I-type header. Experimental results showed that the vapor from side microchannels would flow back into the central microchannel and block the flow through it when the heat flux is high, named mirage flow restraint. Conversely, Kurose et al. [10] explored the characteristics of flow distribution in unequally heated two parallel channels by experimental method. They developed correlation equations to predict mass flow rates and inlet vapor qualities in each channel under uneven heating conditions. With the development of computer technology, more numerical simulations are carried out to reveal abundant local

* Corresponding author.
E-mail addresses: yang2762473445@stu.xjtu.edu.cn (P. Yang), bleach_miku@163.com (W. Ling), tianke120637@stu.xjtu.edu.cn (K. Tian), zengmin@mail.xjtu.edu.cn (M. Zeng), wangqw@mail.xjtu.edu.cn (Q. Wang).

https://doi.org/10.1016/j.energy.2023.126957
Received 14 March 2022; Received in revised form 15 January 2023; Accepted 14 February 2023
Available online 14 February 2023

Nomenclature

A	Heat transfer area (m^2)
AR	The dimensionless flow area ratio (1)
Bo	Boiling number (1)
D_h	The hydraulic diameter (m)
E	Correction factor (1)
f	Darcy friction coefficient (1)
Fr	Froude number (1)
g	Gravitational acceleration (m/s^2)
G	Mass velocity ($kg/(m^2 \cdot s)$)
h	Specific enthalpy (J/kg)
H	The thermal non-uniformity dimensionless parameter (1)
K	Local resistance coefficient (1)
L	Length (m)
m	Mass flow rate of channel (kg/s)
M	Total mass flow rate (kg/s)
M_r	Molar mass (kg/kmol)
n	Channel number
P	Pressure (Pa)
p_r	Relative pressure (1)
q	Heat flux (W/m^2)
Q	Volume flow rate (m^3/s)
R	Correction factor (1)
Re	Reynolds number (1)
R_i	Mass flow rate ratio (1)
T	Temperature (K)
v	Flow velocity (m/s)
W	Thermal power (W)
We	Weber number (1)
x	Vapor quality (1)
X_{tt}	Martinelli number (1)
Y	Flow non-uniformity dimensionless parameter (1)
Y_m	Dimensionless parameter (1)

Greek symbols

α	Heat transfer coefficient ($W/(m^2 \cdot K)$)
θ	Tilt angle (°)
λ	Thermal conductivity ($W/(m \cdot K)$)
μ	viscosity (Pa·s)
ρ	Density (kg/m^3)
σ	surface tension coefficient (N/m)
ϕ	The friction correction factor (1)

Subscripts

br	Side branch channel
f	Frictional
G	Saturated gas phase and liquid phase
GO	The two-phase flow is regarded as the gas flow with the equal mass flow rate
i	i-th
in	Inlet
L	Saturated liquid phase
LO	The two-phase flow is regarded as the liquid flow with the equal mass flow rate
m	Mass average
out	Outlet
st	Straight passage
us	Upstream

characteristics. Minocha and Joshi [11] revealed the effects of turbulent parameters (k and ε) on pressure drop and flow maldistribution by using 3D simulation. They suggested placing perforated baffles in the parallel flow system to reduce the vortex flow, which is good for flow uniformity. Zhou et al. [12] numerically investigated the roles of several modified methods on flow distribution in a multi-channel heat exchanger. The results showed that improved double-inlet could reduce pressure drop (29.62%) and improve flow distribution (66.36%). Zheng et al. [13] studied the flow uniformity at the entrance of LNG (liquefied natural gas) heat exchangers using FLUENT, and they found that the flow distribution is more sensitive to gas flow velocity than liquid flow velocity. Tan et al. [14] proposed a spider netted microchannel network, which can improve the temperature and flow distribution when the heat flux is non-uniform. Zhou et al. [15] investigated the flow area ratio on flow uniformity, and they concluded that when the flow area ratio between the inlet header and outlet header is smaller than 1, flow distribution will be worsened.

Unfortunately, experimental methods and traditional CFD methods are difficult to investigate the flow distribution and heat transfer in the complex parallel flow system with many heat transfer channels, which requires tremendous economic cost and time cost. Actually, even simulating the two-phase flow of simple multi-channel heat exchangers requires a long calculation period due to the complexity of capturing the phase interface, which is not beneficial to the two-phase flow heat exchanger design. Therefore, a fast and accurate method to predict flow distribution and heat transfer of two-phase flow in the parallel flow system is required to design the system. Cross [16] established a flow network to simulate the flow distribution in pipe networks. Camilleri et al. [17] proposed a flow distribution prediction model for compact heat exchangers based on Kirchhoff's law and introduced the channel to header area ratio to analyze flow distribution. Bava and Furbo [18] presented a model for single-phase flow distribution in the solar collector using pressure drop correlations. They pointed out that turbulent flow in the header can improve the flow maldistribution. García-Guendulain et al. [19] developed a theoretical model to analyze the flow uniformity in a flat plate collector using the conservations of mass and momentum. Moreover, they extended the theoretical model to simulate the flow characteristics in large solar collector networks and found that the flow non-uniformity of the solar network will be reduced when the channel to header area ratio is less than 0.25. Similarly, Bava and Furbo [20] established a modified TRNSYS-Matlab model for large solar collector fields through coupling flow distribution theoretical model. Unlike the single-phase flow problem mentioned above, the flow distribution of two-phase flow is more difficult to predict. Lee and Jeong [21] proposed a numerical model for multi-port heat exchangers considering phase distribution in the header. Mahvi and Garimella [22] developed a new model to predict liquid and vapor mass flow rates in each branch of the condenser based on the flow pattern in the header. However, the effect of unequal heating on flow distribution wasn't discussed in their investigation. Huang et al. [23] presented an analytical model to calculate the flow distribution in proton exchange membrane fuel cell stacks using the flow network method, and the effect of two-phase flow in the unit cell on the flow distribution was quantitatively studied. Aka and Narayan [24] established a numerical model to predict the transient flow distribution of two-phase flow by MATLAB Simulation, but they did not consider the effect of headers.

It can be seen from the above literature that investigations on flow distribution in a complex parallel flow system are usually focused on single-phase flow, and the pressure drops of two-phase flow in the header are often neglected in the above theoretical models. Besides, the effect of non-uniform heating on two-phase flow maldistribution and heat transfer is rarely studied. Therefore, a numerical model is established in this study to quickly predict the flow distribution and thermal performance of two-phase flow in a parallel flow system. Moreover, the

effects of header and non-uniform thermal load are discussed in detail. This study is expected to be used in heat exchanger design and optimization.

2. Numerical model and validation

As shown in Fig. 1, the parallel flow heat exchange system consists of several parallel channels connected by the inlet and outlet header. According to the flow direction, parallel flow heat exchangers can be divided into U-type and Z-type, and others can be regarded as a combination of these two types, such as H-type. The flow directions in the inlet and outlet header of the U-type exchanger are opposite. On the contrary, the flow directions in the inlet and outlet header of the Z-type exchanger are the same. H-type exchangers have two inlets and outlets. This study is focused on U-type and Z-type exchangers.

In order to simplify the model, the following reasonable assumptions are proposed in this paper based on practical physical problems.

(1) The flow conditions are steady state;
(2) The axial heat conduction on the branch channel can be ignored;
(3) The heat transfer of the header is not considered, but the pressure drop of that is taken into account;
(4) The simulated parallel flow heat exchangers are symmetrically designed.

2.1. Governing equations

According to the mass conservation, the total mass flow rate of the heat exchanger is equal to the sum of the mass flow rate in all branch channels, thus,

$$M_{\text{total}} = m_1 + m_2 + \ldots + m_i + \ldots + m_n \tag{1}$$

where M and m are mass flow rate (kg/s), n is the total channel number and the subscript i represents the i-th channel. Moreover, as shown in Fig. 2, for a mass node in the heat exchange system, the total mass flowing to the node equals the total mass leaving the node. N is mass flow rate and j is the total number of leaving streams.

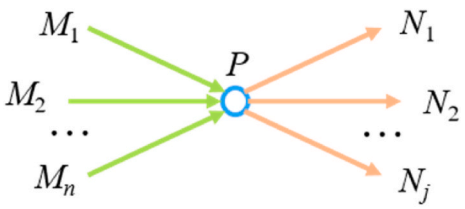

Fig. 2. The mass node P.

$$M_1 + M_2 + \ldots + M_{n-1} + M_n = N_1 + N_2 + \ldots + N_{j-1} + N_j \tag{2}$$

Analogously to Kirchhoff's laws for electrical circuits, in solar collectors as well as in any other parallel flow systems, the total pressure drop of each branch channel is the same. That means equation (3) can be written as follows:

$$P_{in} - P_{out} = (\Delta P_{h\_in})_1 + (\Delta P_{channel})_1 + (\Delta P_{h\_out})_1 = \ldots = (\Delta P_{h\_in})_i + (\Delta P_{channel})_i + (\Delta P_{h\_out})_i \tag{3}$$

where P_{in} and P_{out} are the inlet and outlet pressure of the parallel flow heat exchanger (Pa), and $(\Delta P_{channel})_i$ means the pressure drop between the inlet and outlet of the i-th branch channel. $(\Delta P_{h\_in})_i$ represents the pressure drop between the header inlet and the i-th channel inlet. Similarly, $(\Delta P_{h\_out})_i$ is the pressure drop between the i-th channel outlet and the header outlet. According to the momentum equation, pressure drop can be divided into frictional pressure drop, accelerated pressure drop, gravitational pressure drop and local pressure drop, whose specific formulas are shown in the next section. Moreover, the flow in this study may involve three flow states: subcooled fluid, flow boiling and superheated vapor.

Based on the energy conservation, fluid specific enthalpy and vapor quality can be calculated as follows:

$$qA = (h_{out} - h_{in})m \tag{4}$$

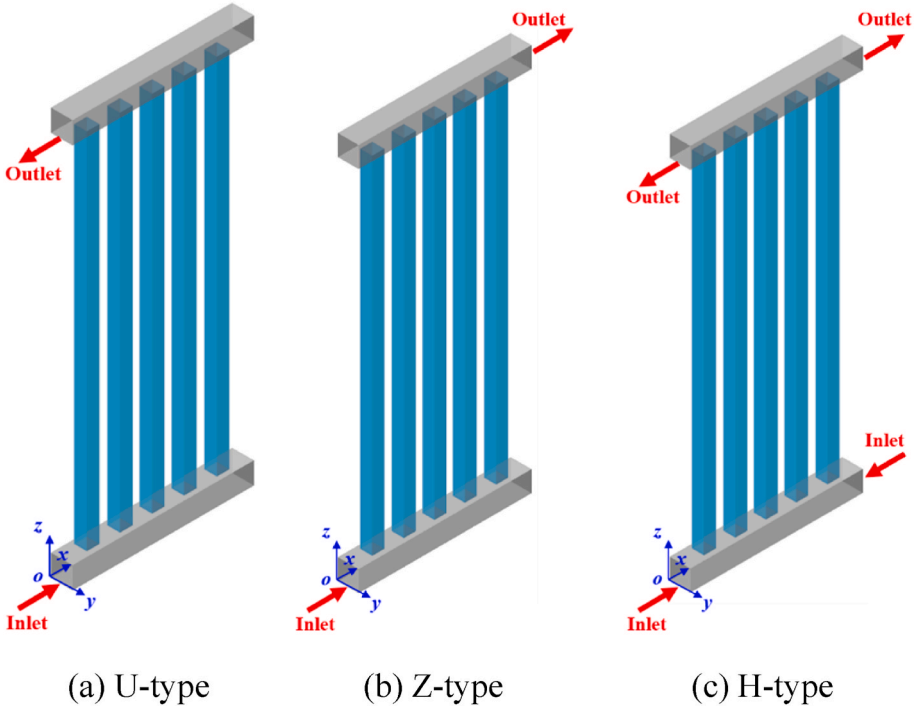

Fig. 1. 3D model of typical parallel flow heat exchangers.

$$x = \frac{h - h_{l-sat}}{h_{lv}} \tag{5}$$

where q is heat flux (W/m^2), A is heat exchange area (m^2), h_{out} and h_{in} (J/kg) are outlet and inlet specific enthalpy of one segment. x is vapor quality (1), $h_{l\text{-}sat}$ is the specific enthalpy of saturated liquid and h_{lv} is the latent heat.

2.2. Pressure drop and heat transfer correlations

2.2.1. Frictional pressure drop and heat transfer of single-phase flow

From fluid dynamics knowledge [25], the frictional pressure drop of single-phase flow can be written as follows:

$$\Delta P_f = f\left(\frac{1}{2}\rho v^2\right)\frac{L}{D_h} \tag{6}$$

where ΔP_f is frictional pressure drop (Pa), ρ is density (kg/m^3), v is flow velocity (m/s), L and D_h are path length and hydraulic diameter (m). F is Darcy friction coefficient. If the fluid flow is laminar, the flow is divided into the developing flow and the fully developed flow depending on the distribution of the boundary layer. Correspondingly, when the flow is the fully developed flow, the friction coefficient is given as Eq. (7) [25].

$$f = \frac{64}{\mathrm{Re}} \tag{7}$$

where Re is Reynolds number. L_{in} is introduced to describe the length of entrance flow, which depends on Reynolds number and hydraulic diameter [26], as follows:

$$L_{in} = 0.05\mathrm{Re}D_h \tag{8}$$

The friction coefficient in the developing flow f_{in} is calculated as Eq. (9) [27].

$$f_{in} = 4 \times 7.495\left(\frac{L_{in}/D_h}{\mathrm{Re}}\right)^{0.6189} \Big/ \left(L_{in}/D_h\right) \tag{9}$$

Therefore, when the fluid flow is laminar, the frictional pressure drop is expressed by Eq. (10).

$$\begin{cases} \Delta P_f = f_{in}\left(\frac{1}{2}\rho v^2\right)\frac{L}{D_h} & L < L_{in} \\ \Delta P_f = \left[f_{in}L_{in} + f(L - L_{in})\right]\left(\frac{1}{2}\rho v^2\right)\frac{1}{D_h} & L > L_{in} \end{cases} \tag{10}$$

Besides, when the fluid flow is turbulent, the influence of the entrance section can be negligible and the friction coefficient is given as Eq. (11) [25].

$$f = 0.3164\mathrm{Re}^{-0.25} \tag{11}$$

As for the heat transfer of single-phase flow, Gnielinski formula [28] is accurate enough to predict the heat transfer in the channel [28], which is defined as follows:

$$Nu = \frac{(f/8)(\mathrm{Re} - 1000)\mathrm{Pr}}{1 + 12.7\sqrt{f/8}\left(\mathrm{Pr}^{2/3} - 1\right)}\left[1 + \left(\frac{L}{D_h}\right)^{2/3}\right] \tag{12}$$

$$\alpha = (Nu\lambda)/D_h \tag{13}$$

where Pr, α and λ are Prandtl number, heat transfer coefficient (W/(m^2·K)) and thermal conductivity (W/(m·K)), and f is given as Eq. (11).

2.2.2. Frictional pressure drop and heat transfer of two-phase flow

According to the study of Whalley [29], when the ratio of liquid and gas viscosity is less than 1000, Friedel model [30] is recommended to calculate the frictional pressure drop of two-phase flow, which is given as follows:

$$\Delta P_f = \phi_{LO}^2 \Delta P_{LO} \tag{14}$$

where ϕ_{LO}^2 is the friction correction factor, and subscript "LO" represents that the two-phase flow is regarded as the liquid flow with equal mass flow rate. ΔP_{LO} is the frictional pressure drop in liquid flow, which can refer to the formulas in the previous section.

$$\phi_{LO}^2 = A_1 + \frac{3.24A_2A_3}{Fr^{0.045}We^{0.035}} \tag{15}$$

$$A_1 = (1 - x)^2 + x^2\left(\frac{\rho_L f_{GO}}{\rho_G f_{LO}}\right) \tag{16a}$$

$$A_2 = x^{0.78}(1 - x)^{0.224} \tag{16b}$$

$$A_3 = \left(\frac{\rho_L}{\rho_G}\right)^{0.91}\left(\frac{\mu_L}{\mu_G}\right)^{0.19}\left(1 - \frac{\mu_L}{\mu_G}\right)^{0.7} \tag{16c}$$

$$Fr = \frac{G^2}{gD_h\rho_m^2} \tag{17a}$$

$$We = \frac{G^2D_h}{\rho_m\sigma} \tag{17b}$$

$$\rho_m = 1 \Big/ \left(\frac{x}{\rho_G} + \frac{1 - x}{\rho_L}\right) \tag{17c}$$

where subscript "GO" means that the two-phase flow is considered the gas flow with an equal mass flow rate. Subscripts "G" and "L" mean saturated gas phase and saturated liquid phase. x is vapor quality (1), and f is friction factor, obtained in section 2.2.1. μ, G, σ and g are viscosity (Pa·s), mass velocity (kg/(m^2·s)), surface tension coefficient (N/m) and gravitational acceleration (m/s^2). Fr and We are Froude number and Weber number. ρ_m is the average density of two-phase flow, so the gravitational pressure drop of two-phase flow is shown below:

$$\Delta P_g = \rho_m g L \sin\theta \tag{18}$$

where θ is the tilt angle.

For the sake of heat transfer simulation, Gungor-Winterton model [31] is used to calculate the heat transfer in two-phase flow.

$$\alpha = E\alpha_l + R\alpha_b \tag{19}$$

where E and R are correction factors, and α_l is the heat transfer coefficient of liquid phase, which is determined by using Gnielinski formula Eq. (12) and Eq. (13).

$$\alpha_b = \frac{55q^{0.67}p_r^{0.12}}{\sqrt{M_r}}\left(0.434\ln\frac{1}{p_r}\right)^{-0.55} \tag{20}$$

where p_r is relative pressure, defined as the ratio of pressure to critical pressure. M_r is molar mass (kg/kmol).

$$E = 1 + 24000Bo^{1.16}\frac{1.37}{X_{tt}^{0.86}} \tag{21}$$

where Bo and X_{tt} are boiling number and Martinelli number. They are defined below:

$$Bo = \frac{q}{Gh_v} \tag{22a}$$

$$X_{tt} = \left(\frac{1 - x}{x}\right)^{0.9}\left(\frac{\rho_g}{\rho_l}\right)^{0.5}\left(\frac{\mu_l}{\mu_g}\right)^{0.1} \tag{22b}$$

Based on the calculation of E, R can be calculated as follows:

$$R=\frac{1}{1+1.15\times10^{-6}E^{2}\mathrm{Re}_{l}^{1.17}} \tag{23}$$

where Re_l is Reynolds number of the liquid phase.

2.2.3. Local pressure drop

Undoubtedly, the flow characteristics of the header have significant effects on flow distribution in parallel flow systems. As shown in Fig. 3, the local pressure losses discussed in the connection between the header and the branch channel are given as follows:

$$\begin{aligned}P_f-P_m&=\Delta P_{\mathrm{br}}=K_{\mathrm{br}}\left(\frac{1}{2}\rho {v_{\mathrm{st}}}^2\right)\\ P_f-P_b&=\Delta P_{\mathrm{st}}=K_{\mathrm{st}}\left(\frac{1}{2}\rho {v_{\mathrm{us}}}^2\right)\end{aligned} \tag{24}$$

where K is the local resistance coefficient. Subscripts "us", "br" and "st" mean upstream, side branch channel and straight passage.

In this study, the angle between the straight passage of the header and the side branch channel φ is 90°. Besides, the cross-sectional area of header upstream, side branch channel and header straight passage satisfy the relationship that $A_{\mathrm{br}}+A_{\mathrm{st}}>A_{\mathrm{us}}, A_{\mathrm{st}}=A_{\mathrm{us}}$. Therefore, according to the local resistance coefficient reported by Idelchik [32], K_{br} and K_{st} of the diverging wye are expressed respectively as below:

$$\begin{aligned}K_{\mathrm{br}}&=C_1\left[1+\left(\frac{v_{\mathrm{br}}}{v_{\mathrm{us}}}\right)^2-2\frac{v_{\mathrm{br}}}{v_{\mathrm{us}}}\cos\varphi\right]\\ C_1&=1.1-0.7\frac{Q_{\mathrm{st}}}{Q_{\mathrm{us}}}\quad\left(\text{if }\frac{A_{\mathrm{br}}}{A_{\mathrm{us}}}\le0.35,\frac{Q_{\mathrm{st}}}{Q_{\mathrm{us}}}\le0.4\right)\\ C_1&=0.85\quad\left(\text{if }\frac{A_{\mathrm{br}}}{A_{\mathrm{us}}}\le0.35,\frac{Q_{\mathrm{st}}}{Q_{\mathrm{us}}}>0.4\right)\end{aligned} \tag{25}$$

where Q is the volumetric flow rate (m^3/s).

$$\begin{aligned}K_{\mathrm{st}}&=C_2\frac{Q_{\mathrm{st}}}{Q_{\mathrm{us}}}\\ C_2&=0.4\quad\left(\text{if }\frac{A_{\mathrm{br}}}{A_{\mathrm{us}}}\le0.4\right)\end{aligned} \tag{26}$$

Moreover, for the converging wye, the loss factors of branch channel and header straight passage are expressed as follows:

$$\begin{aligned}K_{\mathrm{br}}&=C_3\left[1+\left(\frac{Q_{\mathrm{br}}}{Q_{\mathrm{st}}}\frac{v_{\mathrm{st}}}{v_{\mathrm{br}}}\right)^2-2\left(1-\frac{Q_{\mathrm{br}}}{Q_{\mathrm{us}}}\right)^2\right]\\ C_3&=1\quad\left(\text{if }\frac{A_{\mathrm{br}}}{A_{\mathrm{st}}}\le0.35,\frac{Q_{\mathrm{br}}}{Q_{\mathrm{st}}}\le1\right)\end{aligned} \tag{27}$$

$$K_{\mathrm{st}}\approx1.55\frac{Q_{\mathrm{st}}}{Q_{\mathrm{us}}}-\left(\frac{Q_{\mathrm{st}}}{Q_{\mathrm{us}}}\right)^2 \tag{28}$$

2.3. Mathematical model

Based on the governing equations and correlations mentioned in sections 2.1-2.2, a numerical model is established in this study to predict the flow distribution and heat transfer of two-phase flow in the parallel flow system. Fig. 4(a) shows the flow chart of the calculation, and Fig. 4 (b) presents the computational model. The iterative procedure continues until the maximum relative deviation of the total mass flow rate is less than 10^{-3}. Besides, the flow in this model should be divided into three main sections: a section where the subcooled fluid is heated, a section of flow boiling and a section where the fluid is superheated vapor. Furthermore, the flow boiling problem is more complex than single-phase flow, where flow pattern is variable and vapor quality changes

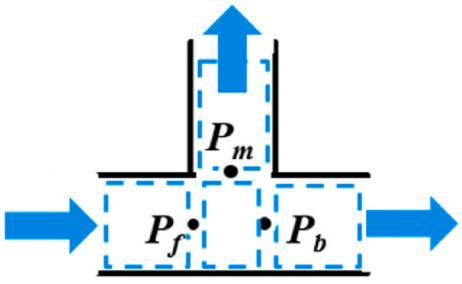

Fig. 3. A distribution part of the header.

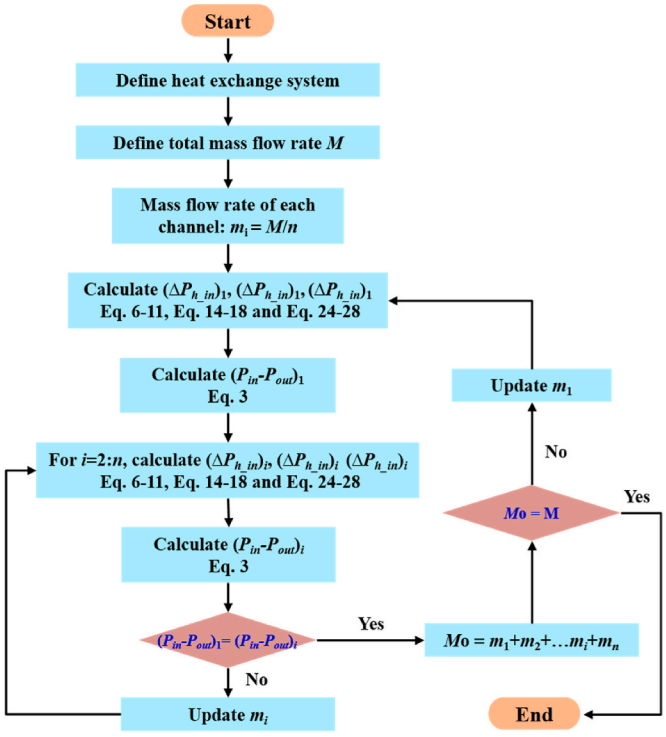

(a) Flow chart of the mathematical model.

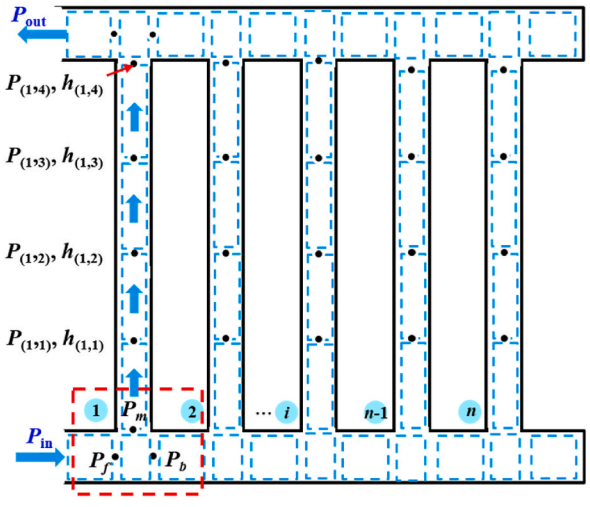

(b) Computational model

Fig. 4. Mathematical model: (a) Flow chart of the mathematical model; (b) Computational model.

along the flow direction. Therefore, it can be seen from Fig. 4(b) that the computational model needs to be discretized to simulate complex operating conditions and improve accuracy. As shown in Fig. 4(b), the fluid state is defined at the segment node. The pressure and specific enthalpy are obtained by iteratively solving pressure drop correlations and energy equations. Once the pressure and specific enthalpy are obtained, other thermophysical properties can be determined. Moreover, the average density of two-phase flow is calculated by Eq. (17c).

2.4. Model validation

For the sake of model validation, the simulation results are compared with the experimental data from Wang et al. [5] and Baikin et al. [33]. The computational model is shown in Fig. 4(b), and the operating parameters and geometrical information are shown in Table 1. Fig. 5 compares the simulated flow distribution with the experimental data from Wang et al. [5] (Total mass flow rate $M = 0.033$ kg/s; channel number $n = 9$). It can be seen that the numerical results agree well with the experimental data and the average relative deviations are 2.9% (Z-type) and 1.7% (U-type). In addition, the comparisons between the predicted flow distribution and experimental results from Baikin et al. [33] (Channel number $n = 3$) are shown in Fig. 6. When the total mass flow rates M are 0.057 and 0.102 kg/s, the average relative deviations are 4.3% and 4.4% respectively. Therefore, the numerical model used in this study is reliable for the following investigation.

3. Results and discussions

3.1. Effect of geometric parameters

3.1.1. Header type

The header is an important component of the parallel flow heat exchange system, which directly affects the flow direction. In order to investigate the effect of header type on flow distribution, two typical structures U-type and Z-type are compared in this section. The geometric parameters of the simulated heat exchangers are the same as those in case 2 (Table 1). The system has nine branch channels, and each channel is uniformly heated with 2000 W. The fluid is water with the inlet temperature of 363 K. The inlet pressure of the parallel flow system is 200 kPa. Therefore, the pressure range of water in this study is within 101–200 kPa, which means the ratio of liquid and gas viscosity is less than 23. As a result, Friedel correlation can be used to calculate the frictional pressure drop of two-phase flow in this study according to the investigation of Whalley [29].

The dimensionless mass flow rate ratio R_i is used to quantify the flow distribution in each channel, defined as the ratio of the mass flow rate in the i-th channel to the total mass flow rate.

$$R_i = \frac{m_i}{M} \tag{29}$$

Besides, a dimensionless parameter Y is introduced to analyze flow non-uniformity, which is expressed as follows:

$$Y = \sqrt{\frac{\sum_i^n (R_i - \overline{R})^2}{n}} \tag{30}$$

where $\overline{R}$ is the arithmetical average of R_i, thus $\overline{R} = 1/n$.

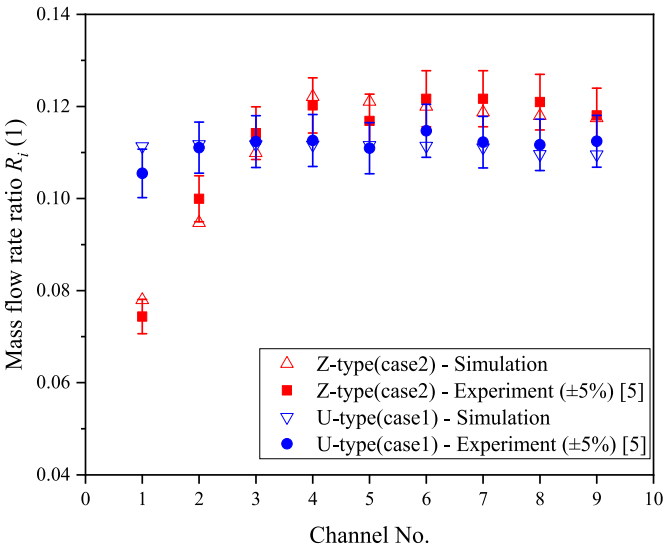

Fig. 5. Model validation with experimental data of Wang et al. [5].

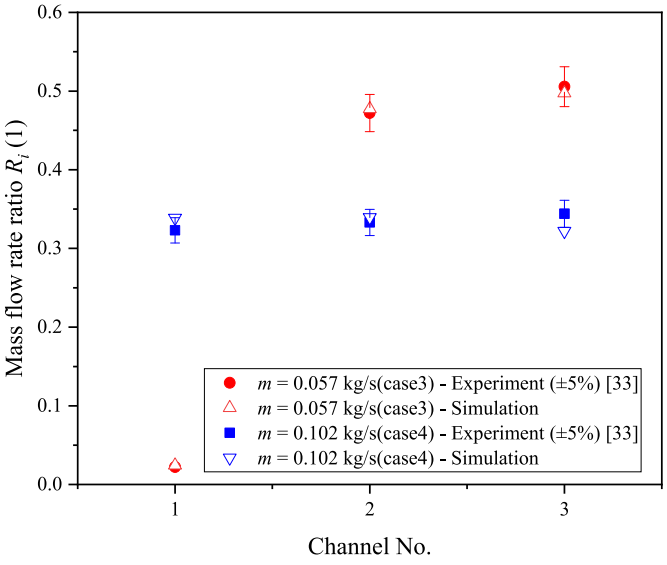

Fig. 6. Model validation with experimental data of Baikin et al. [33].

The flow distributions in two typical heat exchangers (U-type and Z-type) are shown in Fig. 7. It can be seen that the flow distribution in U-type exchanger is more uniform than that in Z-type no matter how the total mass flow rate changes, which is beneficial to heat transfer. Besides, in Z-type heat exchanger, the mass flow rate in the branch channel increases gradually as the branch moves away from the header inlet. On the one hand, the spacing between adjacent branches is small, so the frictional pressure drop of single-phase flow between adjacent branches can be ignored. On the other hand, according to the Bernoulli equation, the decrease of dynamic pressure will increase the static pressure. As a result, the pressure increases along the flow direction in the inlet header,

Table 1
Operating parameters and geometrical information of model validations.

Case	Data from	$D_{channel}$ (mm)	D_{header} (mm)	L (mm)	Total mass flow rate (kg/s)	Channel number	Tilt angle (deg)
1	Ref. [5]	2	12	300	0.033	9	90
2	Ref. [5]	3	12	400	0.033	9	90
3	Ref. [33]	5	19	6000	0.057	3	30
4	Ref. [33]	5	19	6000	0.102	3	30

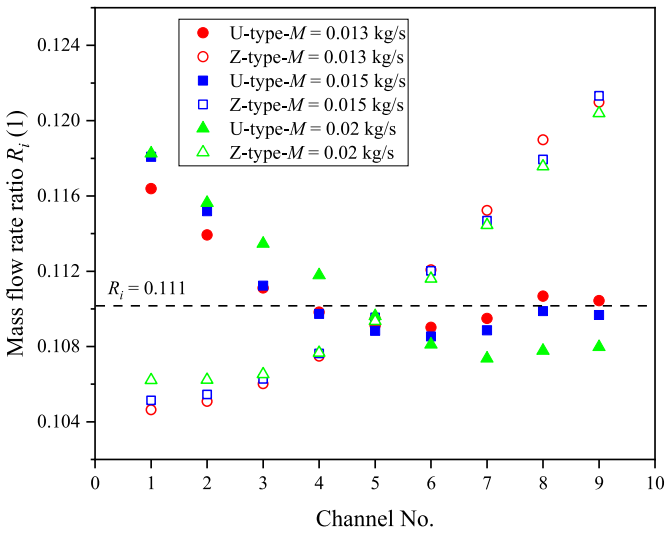

Fig. 7. Flow distribution in different types of parallel flow heat exchange systems.

but decreases in the outlet header. Therefore, the pressure drop between the channel inlet and outlet $(\Delta P_{channel})_i$ increases gradually as the branch moves away from the header inlet in Z-type. But the pressure drop of each channel in U-type is more uniform because the flow direction is opposite in the inlet and outlet header. To quantitatively compare the flow non-uniformity of U-type and Z-type, the dimensionless parameter Y under the above working conditions are presented in Table 2. It is indicated that the flow distribution of Z-type is improved with the increase of the total mass flow rate, but that of U-type is worsened.

3.1.2. Flow area ratio

Except for the header type, the header geometric parameters are also important factors affecting flow distribution, especially the flow area. Therefore, the dimensionless flow area ratio is introduced to investigate its effect on flow distribution in this section. The dimensionless flow area ratio is defined as follows:

$$AR = \frac{n\pi D_h^{\,2}}{4D^2} \tag{31}$$

where D_h is the hydraulic diameter of branch channel, and D is the hydraulic diameter of header. The length and hydraulic diameter of the branch channel are 0.4 m and 0.003 m respectively, and the header length is 0.12 m. The simulations in this section focus on the Z-type exchanger composed of 9 branches, heated uniformly with 2000 W. The inlet temperature and pressure of fluid are 363 K and 200 kPa.

As illustrated in Fig. 8, when the dimensionless flow area ratio AR is 0.22, flow distribution is more uniform than that when AR = 0.79 or 1.30. The mass flow rate in the branch channel no longer monotonically increases as the branch moves away from the header inlet. Furthermore, it can be seen from Fig. 9 that Y increases with increasing AR, which means the decrease in the flow area ratio can improve the flow uniformity of Z-type parallel flow system. On the other hand, when the flow area of branch channels is determined, the smaller AR requires a larger header, which will sacrifice the compactness of system. As shown in Fig. 10, (dY/dAR) is pretty small when AR is less than 0.3, which indicates that the flow maldistribution will not be improved significantly

Table 2
The dimensionless parameter Y in different heat exchange systems.

	M = 0.013 kg/s	M = 0.015 kg/s	M = 0.02 kg/s
U-type	0.0023	0.0031	0.0037
Z-type	0.0057	0.0055	0.0050

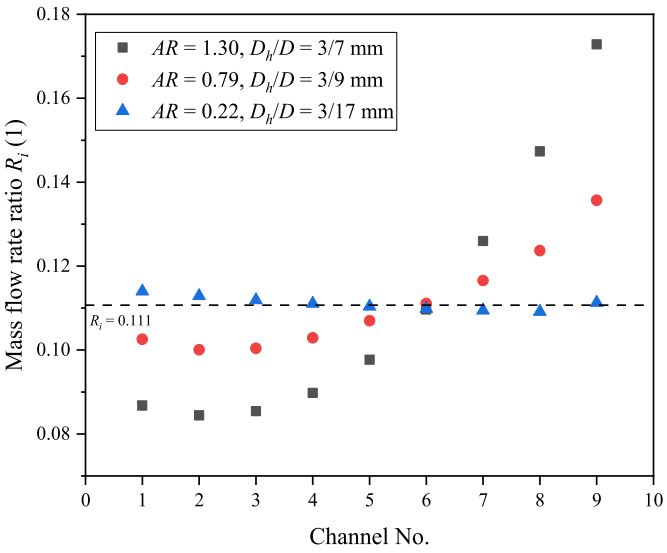

Fig. 8. Flow distribution vary with the dimensionless flow area ratio AR.

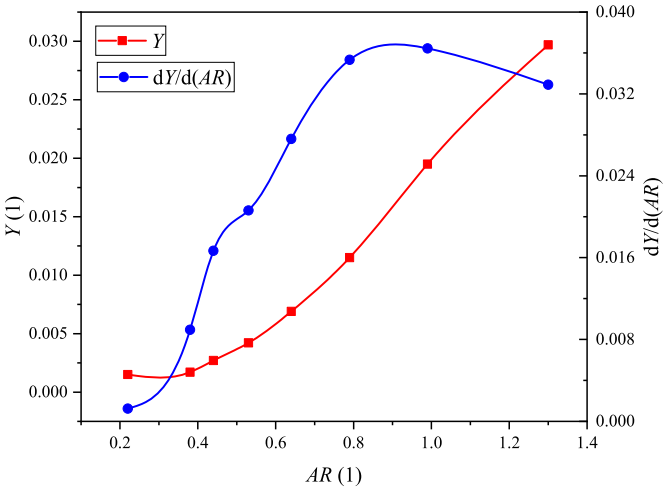

Fig. 9. The dimensionless parameter Y and (dY/dAR) vary with the dimensionless flow area ratio AR.

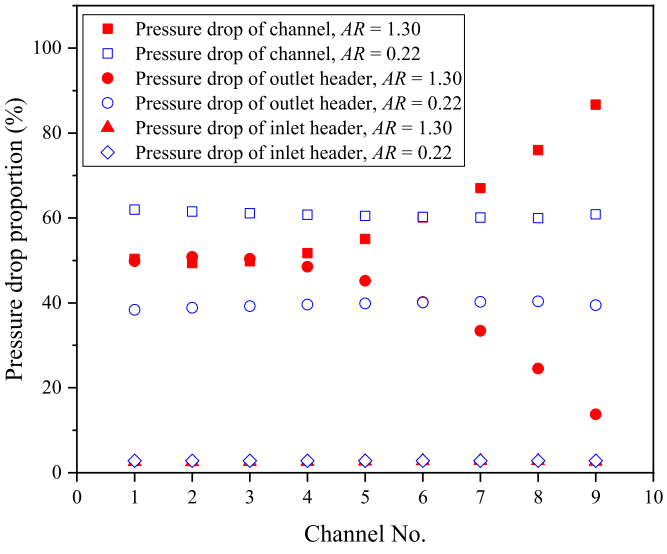

Fig. 10. Pressure drop proportions of the nine channels.

as *AR* decreases when *AR* is less than 0.3. Therefore, decreasing the dimensionless flow area ratio *AR* is beneficial to flow uniformity and heat transfer, but for the sake of the system compactness and production cost, it is not necessary to design *AR* as smaller as possible if *AR* is less than 0.3.

In order to explore the reason why decreasing the dimensionless flow area ratio *AR* can improve the flow distribution in the Z-type parallel flow system, the pressure drop proportions of each channel are presented in Fig. 10. It can be found that the pressure drops of channel and outlet header are the main part of the total pressure drop, so the inlet header pressure drop can be ignored. Besides, when $AR = 0.22$, the proportion of outlet header pressure drop is reduced to about 40%, and the channel loss proportion of each branch is more uniform than that when $AR = 1.30$. In general, the local pressure drop determines the corresponding header pressure drop. As shown in Fig. 11 (a), the local resistance coefficient K_{br} of the converging wye decreases as the channel moves away from the header inlet, so channel loss proportion and mass flow rate increase gradually. Fig. 11 (b) shows K_{br} of the converging wye and the ratio of K_{br} when *AR* is different. It can be seen that although K_{br} increases as *AR* decreases, the ratio of K_{br} between each branch decreases as the *AR* decreases, which means relative values of outlet header pressure drop between each channel are reduced. Therefore, the outlet header loss and channel loss between each branch are more uniform when *AR* decreases, which eventually improves the flow distribution in the system.

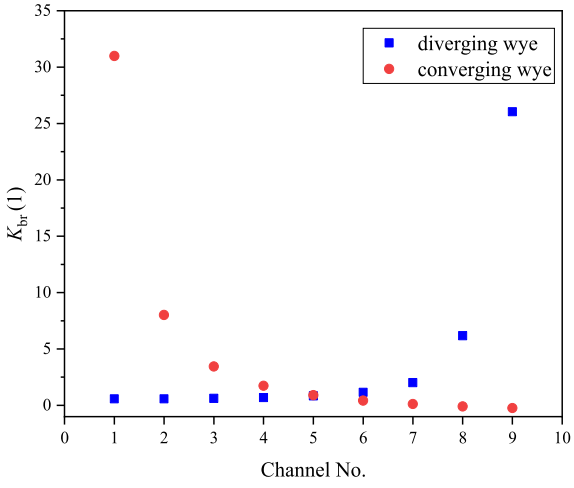

(a) The local resistance coefficient of each branch, $AR = 1.30$.

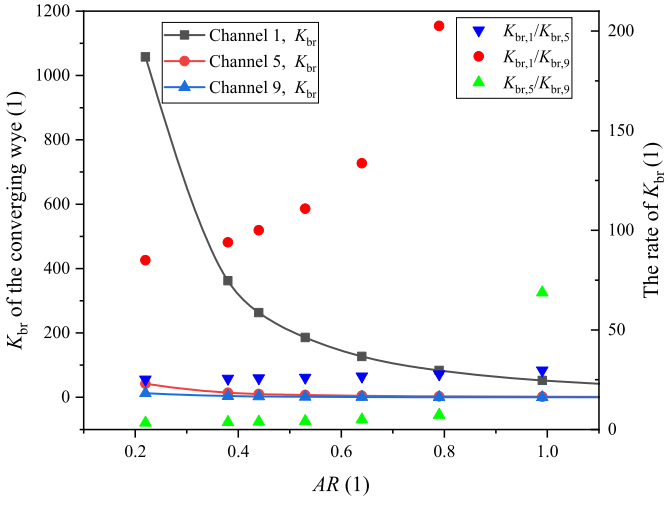

(b) K_{br} of the converging wye and the rate of K_{br} vary with *AR*.

Fig. 11. The local resistance coefficient variation in different conditions.

3.2. Effect of non-uniform heating

In addition to the geometric parameters of the heat exchanger, operating condition is also a significant factor affecting the flow distribution and heat transfer. Some terrible operating conditions should be considered when designing the heat exchanger. Therefore, the effects of non-uniform heating are discussed in the following sections.

3.2.1. The location of the low thermal load channel

Because of the header effect, the location of the low thermal load channel will affect the flow and heat transfer when the system is heated unevenly. Keeping the total mass flow rate $M = 0.015$ kg/s, the total thermal power is 22,000 W, the thermal power of the low thermal load channel is 2000 W, and other channels are heated uniformly. So the thermal load deviation is fixed in this section. Besides, the geometrical dimensions of heat exchange system are the same as those in case 2 (Table 1) and Z-type exchanger is studied. The fluid is water, of which inlet temperature and pressure are 363 K and 200 kPa.

As shown in Fig. 12 (a), it can be found that the mass flow rates of branches near the low thermal load channel are affected significantly, especially the downstream channel. Moreover, it should be mentioned that the mass flow rate deviation increases gradually when the low thermal load channel is away from the header inlet, but the mass flow

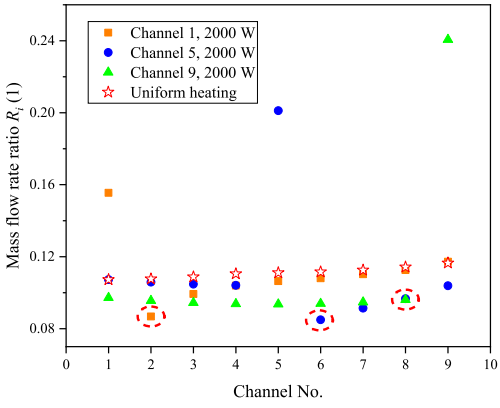

(a) Flow distribution when the location of the low thermal load channel changed.

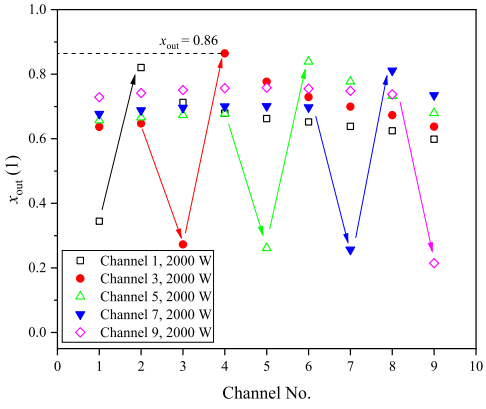

(b) Outlet vapor quality of each channel when the location of the low thermal load channel is different.

Fig. 12. Flow distribution and outlet vapor quality of each channel variation when the location of the low thermal load changed.

rates of channel are not the smallest when the low thermal load channel is channel 9. Furthermore, as illustrated in Fig. 12 (b), the outlet vapor quality of the downstream channel adjacent to the low thermal load channel is the maximum. Besides, $(x_{out})_{max}$ is up to 0.86 when the low thermal load channel is channel 3, but $(x_{out})_{max}$ is only 0.74 when the low thermal load channel is channel 9. Actually, the outlet vapor quality of channel ought to be paid more attention to because once x_{out} is above 1 or a smaller value, heat transfer deterioration may occur in this channel and causes the wall temperature to rise sharply. Therefore, the greater the $(x_{out})_{max}$, the more likely the heat transfer deterioration will occur in the system.

In order to quantitatively investigate the effect of the low thermal load channel location on flow distribution, the dimensionless parameter Y variation is shown in Fig. 13. It is clear that Y increases gradually as the low thermal load channel is away from the header inlet, which means flow distribution is worsened. However, according to the above analysis, the heat transfer performance may not be the worst when the low thermal load channel is channel 9. On the one hand, the mass flow rate of the low thermal load channel is too large, making Y unreasonable. On the other hand, the greater the mass flow rate of the channel, the dryout is less likely to occur. Therefore, the dimensionless parameter Y_m is proposed to evaluate heat transfer characteristics and identify the channel with high risk of heat transfer deterioration. The expression of Y_m is the same as that of Y, but the mass flow rate of the low thermal load channel isn't used. It can be seen from Fig. 13 that Y_m increases firstly and then decreases, and Y_m is the maximum when the low thermal load channel is channel 2, which is the same as the trends of $(x_{out})_{max}$. Overall, the dimensionless parameter Y_m rather than Y is more suitable for non-uniform heating conditions. Moreover, setting channel 2 as the low thermal load channel is the worst operating condition for taking both the flow distribution and heat transfer into account in this study.

3.2.2. Thermal load deviation

Moreover, the thermal load deviation is another significant factor influencing the flow and heat transfer when the system with non-uniform heating. According to section 3.2.1, channel 2 is kept as the low thermal load channel, and other channels are heated uniformly. The dimensionless parameter H is introduced to describe the thermal load deviation, which is given as follows:

$$H = \sqrt{\frac{\sum_{i}^{n} (W_i - \overline{W})^2}{n}} \tag{32}$$

where W is thermal power (W), and $\overline{W} = \frac{W_{total}}{n}$.

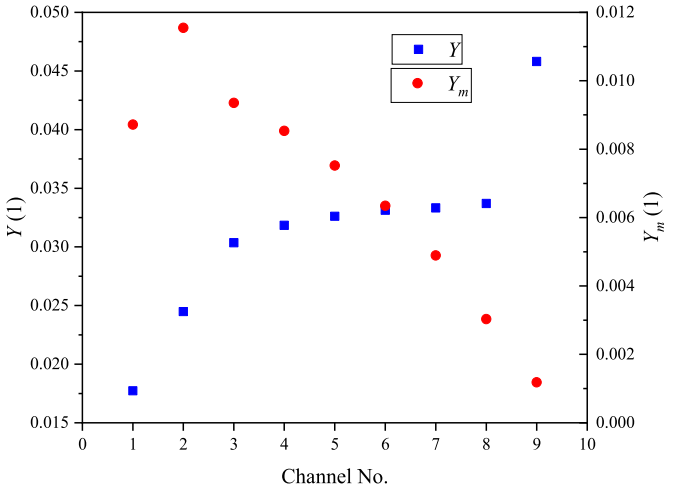

Fig. 13. The dimensionless parameters Y and Y_m vary with the location of the low thermal load channel.

As shown in Fig. 14, it's clearly concluded that the greater H is, the worse the flow distribution is. Moreover, the mass flow rate of channel 3 is the minimum. For analyzing the heat transfer characteristics, the trend of $(x_{out})_{max}$ with the dimensionless parameter H is presented in Fig. 15. It can be seen that the maximum outlet vapor quality $(x_{out})_{max}$ is a linear function of H. This result is helpful for engineers to roughly but quickly predict the worst operating conditions. For example, assuming that $(x_{out})_{max} = 1$ is the worst operating condition, the dimensionless parameter H must be less than about 198.

4. Conclusion

To quickly and accurately simulate the flow distribution and heat transfer performance of two-phase flow in the parallel flow system, a numerical model is established in this study. Moreover, the effects of geometric parameters and non-uniform thermal load are discussed in detail. The main conclusions are drawn as follows.

(1) The ratios of mass flow rate predicted by this model are in good agreement with the experimental data, and the maximum average relative deviation is 4.4%.
(2) The flow distribution in U-type heat exchanger is more uniform than that in Z-type exchanger due to the header effect.
(3) Decreasing the channel to header area ratio AR is beneficial to the flow uniformity of Z-type heat exchanger, but for the sake of the system compactness and production cost, it is not necessary to let AR be as smaller as possible when AR is less than 0.3.
(4) Non-uniform heating will worsen the flow distribution because the pressure drop of two-phase flow is sensitive to heat flux. The mass flow rate of branch channels near the low thermal load channel reduced significantly, especially the downstream channel.
(5) Unlike uniform heating conditions, a dimensionless parameter Y_m is defined to evaluate the flow distribution for non-uniform heating conditions. It should be avoided to set the channel 2 as the low thermal load channel in this study for taking both the flow distribution and heat transfer into account.
(6) The dimensionless parameter H is introduced to predict the worst operating condition. The outlet vapor quality $(x_{out})_{max}$ is a linear function of H, which is helpful for engineers to predict the worst operating conditions quickly. If it is assumed that $(x_{out})_{max} = 1$ is the worst operating condition, the thermal non-uniformity dimensionless parameter H must be less than about 198 in this study.

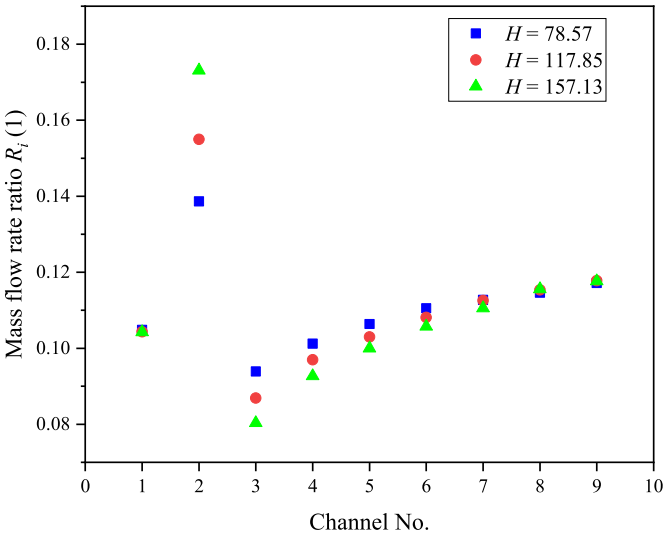

Fig. 14. Flow distribution varies with the dimensionless parameter H.

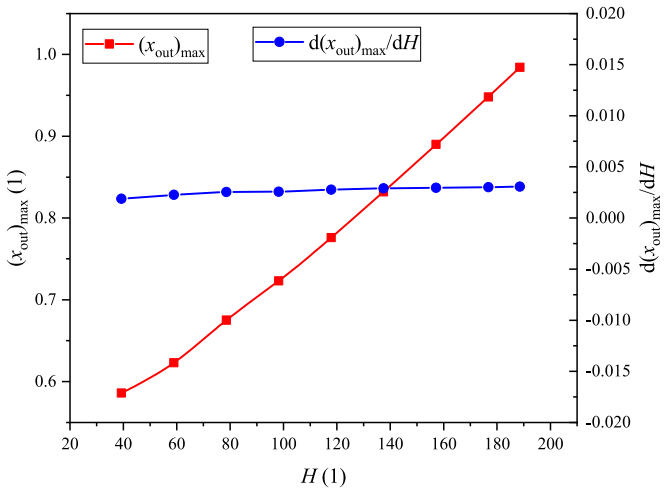

Fig. 15. $(X_{out})_{max}$ varies with the dimensionless parameter H.

This work established a numerical model that can simplify the calculation and predict the flow distribution and heat transfer of the complex parallel flow system, which is significant for the design of two-phase flow system. Conclusions obtained from this study are expected to optimize and design two-phase flow heat exchangers. For the wide application of the present numerical model, considering the effect of flow pattern on flow and heat transfer will be the focus in our future work.

Credit author statement

Ping Yang: Writing - Original Draft, Conceptualization, Methodology, Investigation, Software, Data Curation, Formal analysis and Validation.; **Weihao Ling**: Writing - Review & Editing, Visualization and Formal analysis; **Ke Tian**: Writing - Review & Editing, Formal analysis, Software and Resources; **Min Zeng**: Resources, Data Curation, Writing - Review & Editing and Project administration; **Qiuwang Wang**: Writing - Review & Editing and Supervision.

Declaration of competing interest

The authors declare that they have no known competing financial interests or personal relationships that could have appeared to influence the work reported in this paper.

Data availability

Data will be made available on request.

Acknowledgments

This study is financially supported by the key project of National Natural Science Foundation of China (No. 52130609).

References

[1] Olabi AG, Onumaegbu C, Wilberforce T, et al. Critical review of energy storage systems. J Energy 2021;214:118987.
[2] Chiou JP. The effect of nonuniform fluid flow distribution on the thermal performance of solar collector. Sol Energy 1982;29(6):487–502.
[3] Dong Z, Pan Y, Zhang Z, et al. Model-free adaptive control law for nuclear superheated-steam supply systems. J Energy 2017;135:53–67.
[4] Hu C, Wang R, Yang P, et al. Numerical investigation on two-phase flow heat transfer performance and instability with discrete heat sources in parallel channels. Energies 2021;14(15):4408.
[5] Wang CC, Yang KS, Tsai JS, et al. Characteristics of flow distribution in compact parallel flow heat exchangers, part I: typical inlet header. Appl Therm Eng 2011;31(16):3226–34.
[6] Wang CC, Yang KS, Tsai JS, et al. Characteristics of flow distribution in compact parallel flow heat exchangers, part II: modified inlet header. Appl Therm Eng 2011;31(16):3235–42.
[7] Siddiqui OK, Al-Zahrani M, Al-Sarkhi A, et al. Flow distribution in U-and Z-type manifolds: experimental and numerical investigation. Arabian J Sci Eng 2020;45(7):6005–20.
[8] Klugmann M, Dąbrowski P, Mikielewicz D. Flow distribution and heat transfer in minigap and minichannel heat exchangers during flow boiling. Appl Therm Eng 2020;181:116034.
[9] Kumar R, Singh G, Mikielewicz D. Effect of asymmetric fluid flow distribution on flow boiling in a microchannel heat sink-an experimental investigation. Appl Therm Eng 2022:118710.
[10] Kurose K, Miyata K, Hamamoto Y, et al. Flow boiling heat transfer and flow distribution of HFC32 and HFC134a in unequally heated parallel mini-channels. Int J Refrig 2020;119:305–15.
[11] Minocha N, Joshi JB. 3D CFD simulation of turbulent flow distribution and pressure drop in a dividing manifold system using openfoam. Int J Heat Mass Tran 2020;151:119420.
[12] Zhou J, Ding M, Bian H, et al. Characteristics of flow distribution in central-type compact parallel flow heat exchangers with modified inlet and header. Appl Therm Eng 2020;166:114636.
[13] Zheng W, Jiang Y, Cai W, et al. Numerical investigation on the distribution characteristics of gas-liquid flow at the entrance of LNG plate-fin heat exchangers. Cryogenics 2021;113:103227.
[14] Tan H, Du P, Zong K, et al. Investigation on the temperature distribution in the two-phase spider netted microchannel network heat sink with non-uniform heat flux. Int J Therm Sci 2021;169:107079.
[15] Zhou J, Ding M, Bian H, et al. CFD simulation for the effect of the header match on the flow distribution in a central-type parallel heat exchanger. Chem Eng Res Des 2018;136:144–53.
[16] Cross H. Analysis of flow in networks of conduits or conductors. University of Illinois at Urbana Champaign, College of Engineering, Engineering Experiment Station; 1936.
[17] Camilleri R, Howey DA, McCulloch MD. Predicting the flow distribution in compact parallel flow heat exchangers. Appl Therm Eng 2015;90:551–8.
[18] Bava F, Furbo S. A numerical model for pressure drop and flow distribution in a solar collector with U-connected absorber pipes. Sol Energy 2016;134:264–72.
[19] García-Guendulain JM, Riesco-Ávila JM, Picón-Núñez M. Reducing thermal imbalances and flow nonuniformity in solar collectors through the selection of free flow area ratio. Energy 2020;194:116897.
[20] Bava F, Furbo S. Development and validation of a detailed TRNSYS-Matlab model for large solar collector fields for district heating applications. Energy 2017;135:698–708.
[21] Lee WJ, Jeong JH. Development of a numerical analysis model for a multi-port mini-channel heat exchanger considering a two-phase flow distribution in the header. Part I: numerical modeling. Int J Heat Mass Tran 2019;138:1264–80.
[22] Mahvi AJ, Garimella S. Modeling framework to predict two-phase flow distribution in heat exchanger headers. Int J Refrig 2019;104:65–75.
[23] Huang F, Qiu D, Xu Z, et al. Analysis and improvement of flow distribution in manifold for proton exchange membrane fuel cell stacks. Energy 2021;226:120427.
[24] Aka T, Narayan S. Transient behavior and maldistribution of two-phase flow in parallel channels. IEEE Trans Compon Packag Manuf Technol 2022;12(2):270–9.
[25] Jing SR, Zhang MY. Fluid mechanics. Xi'an, China: Xi'an Jiaotong University Press; 2001.
[26] Kays WM, Crawford ME, Weigand B. Convective heat and mass transfer. New York, USA: McGraw Hill Higher Education Press; 2012.
[27] Langhaar HL. Steady flow in the transition length of a straight tube. J Appl Mech 1942;9(2):A55–8.
[28] Yang SM, Tao WQ. Heat transfer. fourth ed. Beijing, China: Higher Education Press; 2001.
[29] Whalley PB. Two-phase flow and heat transfer. New York, USA: Oxford University Press; 1996.
[30] Friedel L. In: Improved friction pressure drop correlation for horizontal and vertical two-phase pipe flow[C]//European Two-Phase Flow Group Meeting; 1979. Paper E2, Ispra, Italy.
[31] Gungor KE, Winterton RHS. A general correlation for flow boiling in tubes and annuli. Int J Heat Mass Tran 1986;29(3):351–8.
[32] Idelchik IE. Handbook of hydraulic resistance. fourth ed. Redding, CT, USA: Begell House; 2008.
[33] Baikin M, Taitel Y, Barnea D. Flow rate distribution in parallel heated pipes. Int J Heat Mass Tran 2011;54(19–20):4448–57.